Chin. J. Astron. Astrophys. Vol. 1, No. 5, (2001) 406–410
(http://www.chjaa.org or http://chjaa.bao.ac.cn)

Chinese Journal of Astronomy and Astrophysics

Radio Observations of Sgr B2

Xin-Jie Mao[1,2] ⋆ and Jiang-Tao Su[1]

[1] Department of Astronomy, Beijing Normal University, Beijing 100875
[2] Chinese Academy of Science-Peking University Joint Beijing Astrophysics Center, Beijing 100871

Received 2001 March 27; accepted 2001 May 8

Abstract The ^{13}CO ($J = 1 - 0$) map of the molecular cloud Sgr B2 reveals that the mass center of the molecular cloud nucleus does not coincide with that of compact HII regions which are likely to be the outcome of a shock on the cloud. We find evidence of cloud contraction probably resulting from cloud-cloud collision at subsonic speed.

Key words: ISM: clouds — evolution — ISM: lines and bands

1 INTRODUCTION

For the behavior of a molecular cloud in subsonic collision with another, Mao et al. (1992) have obtained simplified one-dimension traveling wave solutions for a plane-parallel slab. Changing the sign in the transformation of variables in their case, we have the following results,

$$\rho = \frac{1}{2}\left[\sqrt{(N+M)^2 + 2z + 2t} + \sqrt{(N-M+2)^2 + 2z + 2t}\right] - 1\,, \tag{1}$$

$$V = \frac{1}{2}\left[\sqrt{(N+M)^2 + 2z + 2t} - \sqrt{(N-M+2)^2 + 2z + 2t}\right] + 1\,. \tag{2}$$

In Eq. (1), ρ increases with increasing t. Instability is expected to occur in strongly perturbed molecular matter, which would probably lead to contraction of clouds, and hence to formation of stars. In order observationally to test whether there is instability occurring in a cloud in collision with another at subsonic velocity, we made ^{13}CO ($J = 1 - 0$) observations towards Sgr B2. It is an intense thermal radio source located ~ 120 pc from the Galactic center and containing molecular matter as much as $(5-10)\times10^6\,M_\odot$ within its dimension of 20 pc (Scoville et al. 1975); it is also one of the most active regions of massive star formation in the Galaxy. More than ten newly born O-type stars in it have been discovered through observations of radio continuum, and OH, H_2O, H_2CO maser emissions (Benson et al. 1984). Hasegawa et al. (1994) have mapped a region of $480'' \times 340''$ near Sgr B2 in the ^{13}CO ($J = 1 - 0$) line with the Nobeyama 45-m telescope. The data show three features: a "shell" of emission, a "hole" left behind by the shrinking of the inner cavity of the shell and a straight "ridge". So they suggested a scenario that a dense, massive clump collided with an extended less dense molecular cloud complex in the Galactic center region. To further investigate the mechanism of star formation collision, we observed the subsonic collision in the Sgr B2 region.

⋆ E-mail: maoxj@bnu.edu.cn

2 OBSERVATIONS

In October and November 1999, we made ^{13}CO ($J = 1 - 0$) line observations near the molecular cloud nucleus of Sgr B2 with the 13.7-m telescope at the Qinghai Station of Purple Mountain Observatory. The half-power beam width of the telescope is $55''$ at 110.2 GHz, which corresponds to 2.2 pc at Sgr B2. Its main beam efficiency is 0.65, the pointing accuracy is better than $10''$, and the tracking accuracy is better than $5''$. A 1.3 mm cooled superconducting receiver was employed as the front receiver with a double-sideband noise temperature ~ 60 K including the quasi-optical system, and a single-sideband system noise temperature about 250 K. Spectra were taken with a 1024 channel acousto-optical spectrometer having a total band width of 168.6 MHz and a channel spacing of 164.65 kHz (corresponding to a velocity resolution of ~ 0.45 km s^{-1} at 110 GHz), and a frequency resolution 250 kHz (velocity resolution of ~ 0.68 km s^{-1} at 110 GHz). The obtained antenna temperature T already corrected for atmospheric attenuation was converted to $T_{\rm A}^*$, after correcting for the radome and ohmic losses, rearward spillover and scattering. Then $T_{\rm R}^*$, the radiation temperature which is convenient for comparing the observations with theory, is obtained from the equation, $T_{\rm R}^* = \frac{T_{\rm A}^*}{\eta_{\rm fss}}$ for the forward spillover and scattering efficiency $\eta_{\rm fss}$ ($\eta_{\rm fss} = 0.61$ at 110 GHz). The system rms noise level at the spectrum resolution of 0.68 km s^{-1} was 0.1 K (for an integration time of 120 seconds). The observations were made in a position-switching mode with a reference position located $30'$ west and $30'$ north of the map origin. The origin of the mapping grid was $\alpha = 17^{\rm h}44^{\rm m}10^{\rm s}$, $\delta = -28°22'00''$ (1950). We mapped a region $7'$ by $9'$ with a grid spacing of $1'$ and the integration time for each spot was 240 seconds.

3 RESULTS AND DISCUSSION

3.1 Spectra of the ^{13}CO ($J = 1 - 0$) Emission

The observed velocity structure of the molecular cloud near Sgr B2 is complicated. Emission together with absorption is common within a velocity span of at least ± 50 km s^{-1} around $V_{\rm LSR} \sim 60$ km s^{-1}, the nominal velocity of the Sgr B2 molecular cloud core. Moreover, the line core velocities of emission at the (0, 4), (0, 0) and (0, –4) positions, whose coordinates are $\alpha = 17^{\rm h}44^{\rm m}10^{\rm s}$, $\delta = -28°18'00''$ (1950), $\alpha = 17^{\rm h}44^{\rm m}10^{\rm s}$, $\delta = -28°22'00''$ (1950) and $\alpha = 17^{\rm h}44^{\rm m}10^{\rm s}$, $\delta = -28°26'00''$ (1950), respectively, are $V_{\rm LSR} = 62$ km s^{-1}, $V_{\rm LSR} = 55$ km s^{-1} and $V_{\rm LSR} = 50$ km s^{-1}, respectively; these values show that there is a decrease in the line center velocity to the extent of $\Delta V \sim 12$ km s^{-1} and therefore a mean gradient value $\frac{\Delta V}{l({\rm pc})} \sim 0.75$ km s^{-1} pc^{-1}. The complicated velocity structure is possibly caused by: (1) There are at least three absorption clouds with velocities of 80 km s^{-1}, 65 km s^{-1} and 50 km s^{-1}, respectively (Rogstad et al. 1974), near Sgr B2 discovered by Rogstad et al. (1974) through observing the H_2CO absorption line at 4830 MHz using a synthesis telescope, which result in the absorption around the velocities of 40 km s^{-1}, 65 km s^{-1} and 80 km s^{-1} marked with A, B and C shown in Fig. 1; (2) in the observations of OCS, CH_2C_2H and HNCO molecules (Goldsmith et al. 1981; Churchwell et al. 1983; Churchwell et al. 1986), all the line core velocities varying from 50 km s^{-1} (at $2' - 4'$ south of Sgr B2(M)) (Benson et al. 1984) to 65 km s^{-1} (at $2' - 4'$ north), most of them within the confines of about 4 pc and having the mean velocity gradient $\frac{\Delta V}{l({\rm pc})} \sim 0.9$ km s^{-1} pc^{-1}, which has been interpreted as the rotation of the cloud core (Chaisson et al. 1973) with its mass of about $4 \times 10^4\, M_\odot$ (Goldsmith et al. 1987); (3) the multiple peaks of emission

as the contributions of clouds with multi-components of velocity in the line of sight suggested by Sun et al. (2000), who were, however, unable to explain the line center shift as a whole. On the basis of the observations including ours, it seems that the complicated velocity structure may result from the presence of absorption clouds near Sgr B2 as well as the rotation of the molecular core.

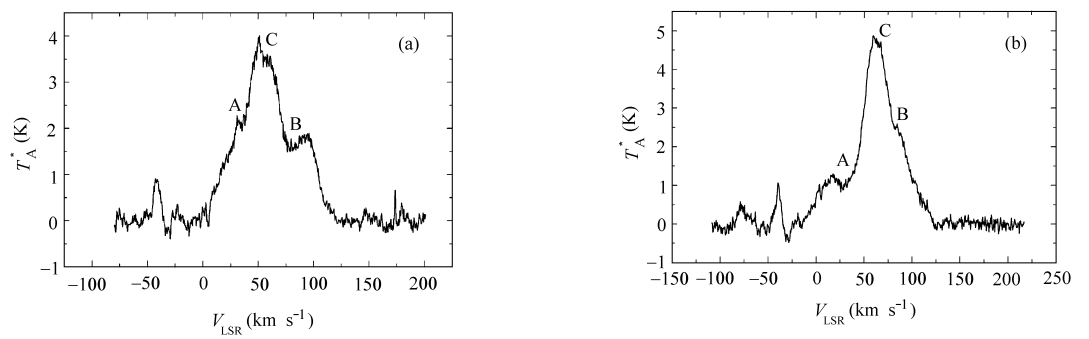

Fig. 1 Spectra of ^{13}CO ($J = 1 - 0$) emission (a) obtained at the (0,0) position, (b) at the (3,2) position. The weak emission at 40 km s^{-1} is present in all the map spectra. A, B and C mark the positions of absorption and the absorption exists in all the map spectra.

3.2 Spatial Distribution of the Molecular Core

Figure 2 is the contour map of integrated intensity ($\int T_R^* dV$) of ^{13}CO ($J = 1 - 0$) emission in the Sgr B2 core. Filled squares indicate some of the locations of the 12 compact HII regions containing many massive newly born stars observed by Benson & Johnston (1984). Distributed in the south-north direction and occurring in a $\sim 2'$ (4 pc) region, they coincide well with the distribution of strong OH and H_2O masers (Rogstad 1974). However, based on our data, the compact HII regions shown in Fig. 2 do not coincide with the regions of the strongest integrated intensities of ^{13}CO ($J = 1 - 0$) emission. Instead, these HII regions are located near the edge of the molecular shell. Loren (1976) hold that the stars formed as a result of collision could be found in the interior or at the edge of the collapsing regions depending on the different times of star formation. Since there is a large-scale cloud collision near Sgr B2 observed by Hasegawa et al. (1994), it is likely that a dense clump might bump into the less dense, extended molecular cloud of Sgr B2 to produce a conic shock that sweeps the gas to form a shell in Sgr B2. Thus, at the edge of the gas shell, which is possibly the edge suggested by Loren, first is the star birth, and then the stellar winds emanating from the newly born stars blow away the gas of the surrounding clouds. In comparison with the maps made by Hasegawa et al., we consider the tail of emission to be the remnants of the shock crossing Sgr B2, as shown on the upper left part of Fig. 2. Note the molecular core in our map is $1'$ larger in the east-west direction than that of Hasegawa et al.(1994).

3.3 Distribution of Subsonic Perturbed Matter and Its Physical Parameters

Figure 3 is the contour map of integrated intensity ($\int T_R^* dV$) of collided matter at a subsonic velocity. When two molecular clouds collide, there is, besides a dominant, supersonic process,

also a subsonic process. In this paper, we only study the latter. The local sound velocity C_0 is defined as $C_0 = \left(\gamma \frac{P}{\rho}\right)^{1/2} \sim \left(\gamma \frac{kT}{m}\right)^{1/2}$, where k, γ and m are the Boltzmann constant, the ratio of specific heats, and the H_2 molecule mass, respectively, and T is the temperature of the molecular cloud. Tentatively adopting $T = 30\,\mathrm{K}$ (Hasegawa 1994), then the local sound velocity is $C_0 = 0.4\,\mathrm{km\ s^{-1}}$. We use Gauss line profiles to fit our data with half-peak width of $1.4\,C_0$, which is assumed to be the unperturbed line width of the molecular cloud. Neglecting other line widening factors, if we set the coordinates on the gas particles in thermal motion, the extra width of the line profile measured in the velocity caused by subsonic perturbation is roughly the sound speed (slightly less than C_0 in the subsonic case) in blue shift side, and here we suppose the cloud is moving towards us to hit the other. The integrated intensity $\int_{V1}^{V2} T_R^* \mathrm{d}V$, where $v_1 = -1.7C_0 = -0.68\,\mathrm{km\ s^{-1}}$ and $v_2 = -0.7C_0 = -0.28\,\mathrm{km\ s^{-1}}$, is thought to relate to the matter affected by the subsonic perturbation. The minimum and maximum integrated intensities in Fig. 3 are $1.45\,\mathrm{K\ km\ s^{-1}}$ and $2.95\,\mathrm{K\ km\ s^{-1}}$, respectively. The contour map of Fig. 3 shows a tendency of the integrated intensity increasing towards the cloud interior. It suggests that the collided cloud at the subsonic velocity tends to contract, which is probably

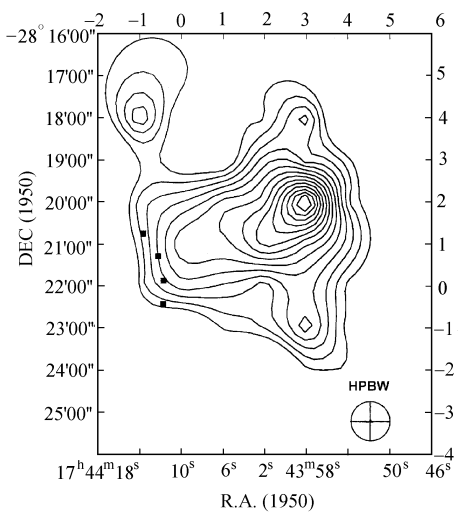

Fig. 2 Contour map of the integrated intensity ($\int T_{\mathrm{R}}^* \mathrm{d}V$) of ^{13}CO ($J = 1 - 0$) emission in the molecular cloud core of Sgr B2 with a grid spacing of $1'$ centered at $\alpha = 17^{\mathrm{h}}44^{\mathrm{m}}10^{\mathrm{s}}$, $\delta = -28°22'00''$ (1950). Contour intervals are $7.6\,\mathrm{K\ km\ s^{-1}}$. The minimum and maximum integrated intensities are $270\,\mathrm{K\ km\ s^{-1}}$, $385\,\mathrm{K\ km\ s^{-1}}$, respectively. The half-power beam width is shown by the cross circle. Filled squares indicate the locations of the compact HII regions observed by Benson & Johnston (1984).

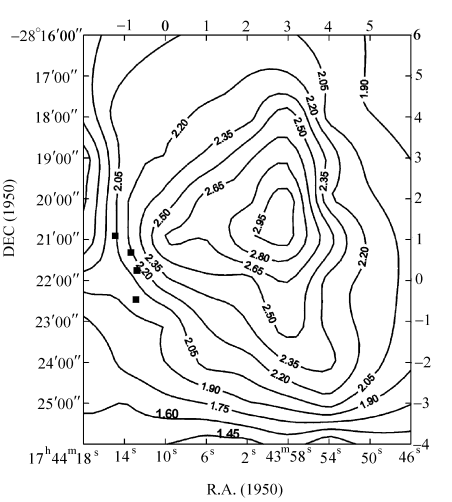

Fig. 3 Contour map of the integrated intensity ($\int T_{\mathrm{R}}^* \mathrm{d}V$) of ^{13}CO ($J = 1 - 0$) emission in Sgr B2. The cloud is perturbed by a collision at a subsonic velocity. Contour intervals are $0.15\,\mathrm{K\ km\ s^{-1}}$. The minimum and maximum integrated intensities are $1.45\,\mathrm{K\ km\ s^{-1}}$ and $2.95\,\mathrm{K\ km\ s^{-1}}$, respectively.

caused by the instability due to the cloud collision. Through the following calculation, we will see that there is a certain amount of matter perturbed at the subsonic velocity. However, in Fig. 3 we do not see the trace of shock impact shown in the upper left part of Fig. 2, because Fig. 3 is a contour map under the subsonic perturbation and the trace of shock, which can be created in supersonic flow, no longer appears.

To calculate the molecular core mass M_1 and its perturbed mass M_2, we assume the excitation temperature $T_{\rm ex} = 30\,{\rm K}$ and use the LTE method (Snell 1988). We introduce the following expressions to calculate the opacity of ^{13}CO ($J = 1 - 0$) emission and the H_2 column density (Nagahama et al. 1998; Sun et al. 2000).

$$\begin{aligned}
\tau(^{13}{\rm CO}) &= -\ln\left\{1 - \frac{T_{\rm R}^*(^{13}{\rm CO})}{5.29[J_1(T_{\rm ex}) - 0.164]}\right\}, \\
N({\rm H_2}) &= 2.13{\times}10^{20}\frac{\int T_{\rm R}^*(^{13}{\rm CO}){\rm d}\nu}{1 - \exp(-5.29/T_{\rm ex})}, \\
J_1(T_{\rm ex}) &= [\exp(5.29/T_{\rm ex}) - 1]^{-1}, \\
M &= \mu {\rm m_H}\int N({\rm H_2}){\rm d}S = \mu {\rm m_H}\sum\nolimits_i S_i N({\rm H_2})_i\,.
\end{aligned}$$

The molecular core size is estimated to be $6' \times 4'$ in Fig. 2. Taking $N({\rm H_2})/N(^{13}{\rm CO}) = 1{\times}10^6$ (Hasegawa et al. 1994), we obtain the average optical depth of the molecular core $\bar{\tau}(^{13}{\rm CO}) = 0.25$, the H_2 column density $N({\rm H_2}) = 4.1{\times}10^{23}\,{\rm cm^{-2}}$, and the core mass $M_1 = 0.9{\times}10^6\,M_\odot$. In contrast, we list the results of Hasegawa et al. $N({\rm H_2}) = 4.5{\times}10^{23}\,{\rm cm^{-2}}$, $M_1 = 1{\times}10^6\,M_\odot$. The perturbed mass M_2 of molecular core amounts to $5.3{\times}10^4\,M_\odot$, about 0.7% of the molecular core mass. Apparently M_1 is greater than M_2, the perturbation at supersonic velocity is dominant. But it is true that some matter is perturbed at subsonic velocity as well.

Acknowledgements We thank Prof. Wu Yuefang for her kind remark which led to improvement of the manuscript.

References

Benson J. M., Johnston K. J., 1984, ApJ, 277, 181
Chaisson E. J., 1973, ApJ, 186, 555
Churchwell E., Hollis J. M., 1983, ApJ, 272, 591
Churchwell F., Wood D., Myers P., Myers R. V., 1986, ApJ, 305, 405
Goldsmith P. F., Linke R. A., 1981, ApJ, 245, 482
Goldsmith P. F., Snell R. L., Hasegawa T. et al., 1987, ApJ, 314, 525
Hasegawa T., Sato F., Whiteoak J. et al., 1994, ApJ, 429, L77
Loren R. B., 1976, ApJ, 209, 466
Mao X. et al., 1992, Chinese Phys. Lett., 9, 165
Nagahama T., Mizuno A., Ogawa H. et al., 1998, AJ, 116, 336
Rogstad D. H., Lockhart I. A., Whiteoak J. B., 1974, A&A, 36, 253
Scoville N. Z., Solomon P. M., Penzias A. A., 1975, ApJ, 201, 352
Snell R. L., Hauang Y. L., Dickman R. L. et al., 1988, ApJ, 325, 853
Sun Jin, Shen Jiajian, Zhang Yangping et al., 2000, Acta Astrophys. Sin., 20(3), 265
Sun Jin, Zhang Yangping, Sun Jinjiang et al., 2000, Journal of Beijing Normal University (Natural Science), 36(4), 517